

Optical-base pressure sensing ability of $\text{Yb}^{3+}:\text{Y}_2\text{Si}_2\text{O}_7$ nanoparticles

Murat Erdem^{*}, Gonul Eryurek^{**} and Baldassare Di Bartolo^{***}

^{*}Department of Physics, Marmara University, Istanbul, TURKEY,

merdem@marmara.edu.tr

^{**}Department of Physics Engineering, Istanbul Technical University, Istanbul, TURKEY,

gozenl@itu.edu.tr

^{***} Department of Physics, Boston College, Boston MA, USA

dibartob@bc.edu

ABSTRACT

We report the drastic dependence on pressure of the spectral output of $\text{Yb}^{3+}:\text{Y}_2\text{Si}_2\text{O}_7$ nanoparticles under IR excitation. The spectrum obtained at atmospheric pressure consisted of an intense blue band. At low pressure the spectrum changed to a broad optical band. The $\text{Y}_2\text{Si}_2\text{O}_7$ activated with Yb^{3+} , since they present bright blue, green and white light emission depending on pressure may be useful as optical-based pressure sensors in potential photonic applications.

Keywords: Pressure effects, Cooperative Emission, White Light

1 INTRODUCTION

The upconversion (UC) emitting materials have numerous application fields in photonics, sensing, security and lasers [1 – 4]. Optical pressure sensors based on the UC emissions from rare earth doped materials are one of the most important applications that can be used to measure the pressure of a distant object. These optical sensors are based on the pressure dependent variation of some spectroscopic properties of the RE^{3+} ions embedded in the host lattice. In particular, the pressure-induced changes in their emission intensities and lifetimes [5], [6] and [7]. The fluorescence intensity (FI) technique takes advantage of the pressure-dependent emission intensities of the emitting levels of the RE^{3+} ion. Another important requirement for the optical sensors based on luminescent ions is that the radiative probabilities of the emitting levels must be high enough to show relatively large emission intensities, being this circumstance closely related to the host lattice in which the RE^{3+} ions are doped. In this context, UC-luminescence based pressure sensing is indeed a hot topic not only in bulk

systems but also in nano-sized emitting systems, in which RE^{3+} -doped fluorescent nano-particles can be used for the pressure measurements via optical processes [8]. Phosphor materials doped with different +3 valence RE^{3+} ions such as glasses, crystals, nanopowders, quantum dots (QD) etc. are candidates to meet these requirements in photonics technology. [9-11]. In particular, among these RE^{3+} -ions

Yb^{3+} doped yttrium silicate hosts are the best candidates due to intense blue emission from Yb^{3+} ions upon 980 nm excitation.

The $\text{SiO}_2\text{-Y}_2\text{O}_3$ (Y_2SiO_5 and $\text{Y}_2\text{Si}_2\text{O}_7$) systems exhibit interesting thermal and luminescence properties that have led to applications in optical memory devices, solid-state laser systems, and phosphors [12]. The host lattice $\text{Y}_2\text{Si}_2\text{O}_7$ shows high thermal, and chemical stability [13]; it has been shown that the structural phases due to its complex high temperature polymorphism are in the γ , z , α , β , γ , and δ forms [14]. However, the main challenge is the represented by preparation of this system as a single-phase material.

The main aim of this work is to investigate the spectral properties of UC-luminescence due to cooperative interactions between the Yb^{3+} ions in Yttrium Silicate nanocrystals upon 950nm laser diode excitation and the possibility of developing an UC-based pressure sensing device.

2 EXPERIMENTAL

2.1. Synthesizes of $\text{Y}_2\text{Si}_2\text{O}_7$ nanocrystals

Nanocrystalline $\text{Y}_2\text{Si}_2\text{O}_7$ powders were synthesized by using the sol-gel method. Precursors with the purity of 99.9% Tetraethyl orthosilicate TEOS, $(\text{Si}(\text{OC}_2\text{H}_5)_4)$, and 99.9% yttrium nitrate hexahydrate $(\text{Y}(\text{NO}_3)_3 \cdot 6\text{H}_2\text{O})$ were used to obtain nanopowders. The SiO_2 and Y_2O_3 mole % ratio was set at 7.0. Yttrium nitrate and TEOS were

separately dissolved in double distilled water and ethanol. The yttrium nitrate salt solution was kept at 70 °C under acidic conditions (1 N HNO₃) for 45 min and then left for cooling at room temperature. After the TEOS solution was added to the solution and stirred for 2.5 h, the mixed solution was placed into circular petri dishes for three weeks to obtain a gel at room temperature. After gelation process, the transparent glass sample was obtained. The glass sample was then heat-treated at at 1050 °C and 1275 °C for 12 h to produce nanocrystalline Y₂Si₂O₇. The samples were prepared with 2.0 mol% Yb ions and they were labeled as YSY1, and YSY2.

2.2. Structural Characterization and Spectroscopic Measurements

X-ray diffraction (XRD) patterns of nanocrystalline powders were collected by Bruker AXS D8 diffractometer for a step size of 0.01°/2θ, between 20 and 90°; using CuKα (λ=1.54184 Å) monochromatic radiation, operating at I=10 mA, V=30 kV. The average particle sizes of the powders were estimated using the Scherrer equation.

$$L = \frac{K\lambda}{\beta \cos \theta} \quad (1)$$

where L is the average size of the ordered (crystalline) domains, K is a dimensionless shape factor that 0.89 for spherical particles (0.89 < K < 1), λ is the X-ray wavelength, β is the width of the peak at half maximum (FWHM) intensity of specific phase in radians, and θ is the center angle of the considered Bragg reflection.

As a further confirmation of the average particle size, SEM images of the samples were obtained by a JEOL 6340F model scanning electron microscope.

Room temperature diffuse reflectance spectra of the powders were obtained in the spectral range 200–1100 nm using Perkin Elmer Model Lambda 35 UV–vis spectrometer to identify the absorption lines of Yb³⁺ ions. The luminescence spectra of the samples were carried out at different environment pressure using a diode laser (Laser Drive Inc.-LDI-820) with a wavelength of 950 nm to excite the nano-powder. The luminescence from the powder was focused onto a Monochromator (McPherson Inc. Model 2051) and detected to a PMT (Hamamatsu R1387 photomultiplier tube with an S20 response) and InGaAs semiconductor detector (Princeton Inc. Model ID-441-C) with a preamplifier (Stanford Res. Model SR560). When examining the cooperative emission, a short wavelength

pass filter (800 nm) was used to avoid the scattered excitation light to enter the monochromator.

The blue emission brightness was recorded by an Allied Scientific Pro ASP-MK350 Model luminance meter to obtain measurements of the International Commission on illumination (CIE) coordinates. All measurements were performed at room temperature.

3 RESULTS AND DISCUSSION

3.1 Structural Characterization

Fig. 1 shows the XRD pattern of the YSY1 and YSY2 powders synthesized by sol–gel method annealed at 1050 °C and 1275°C for 12 h. The triclinic α-Y₂Si₂O₇ phase with the P1̄ space group and the monoclinic γ-Y₂Si₂O₇ phase with the P2_{1/c} space group of the powders were matched by comparing the peak positions and intensities with those in the joint commutation powder diffraction standards (JCPDS) in this study. It can be clearly seen from the figure that the positions of most of the diffraction peaks of YSY1 and YSY2 powder correspond well to the JCPDS cards of α-Y₂Si₂O₇ (PDF380223) and γ-Y₂Si₂O₇ (PDF45-0042) respectively.

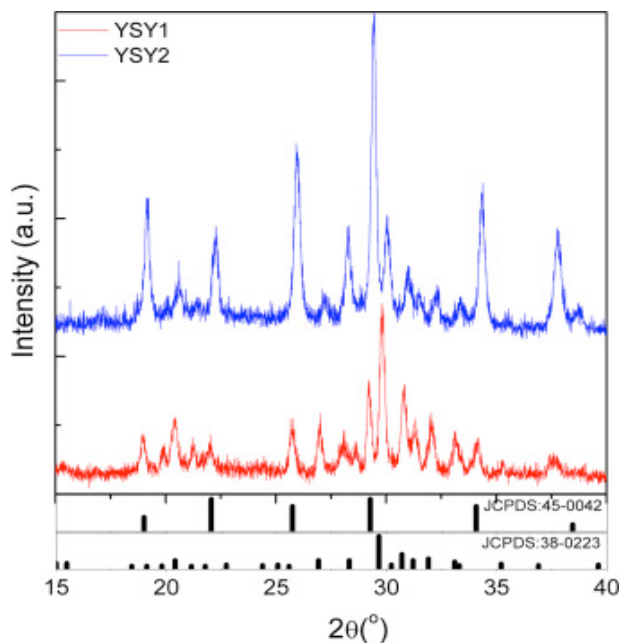


Figure 1 XRD images of α-Y₂Si₂O₇ and γ-Y₂Si₂O₇ powders activated with Yb³⁺.

3.2 Spectroscopic Measurements

Fig. 2 shows the diffuse reflectance spectra of the YSY1 and YSY2 nano-powders in the range of 900–1000 nm. The dip corresponded to transitions from the ${}^2F_{7/2}$ ground state of the Yb^{3+} ion to the ${}^2F_{5/2}$ excited level in the powders. The spectral profile of the dip was observed to change with phase transformation of $\text{Y}_2\text{Si}_2\text{O}_7$ due to the annealing temperature. The strongest absorption corresponding to the deepest dip around 973 nm is related to the transition from the lowest Stark level of the ground level state ${}^2F_{7/2}(0)$ to the lowest Stark level of the excited state ${}^2F_{5/2}(0)$. The other less deep and less separated dips located at around 961.1 nm and 913.5 nm correspond to ${}^2F_{7/2}(0) \rightarrow {}^2F_{5/2}(1)$ and ${}^2F_{7/2}(0) \rightarrow {}^2F_{5/2}(2)$ transitions.

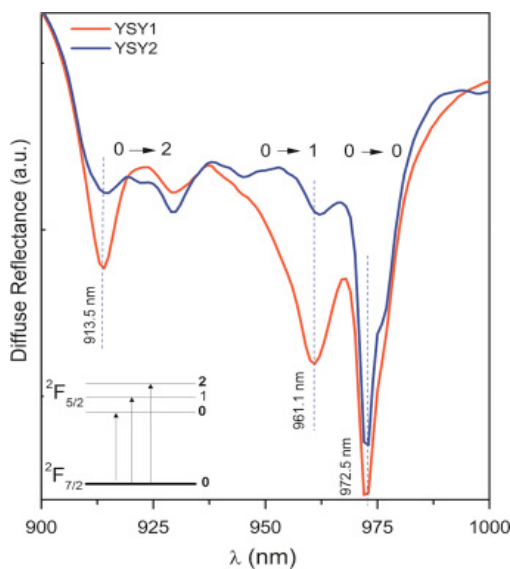


Figure 2 The diffuse reflections spectrum of $\alpha\text{-Y}_2\text{Si}_2\text{O}_7$ and $\gamma\text{-Y}_2\text{Si}_2\text{O}_7$ powders activated with Yb^{3+} powders.

Fig. 3 and 4 present the pressure dependent UC-luminescence spectra of the powders. As it is reported in Fig. 3a and b, its intensity varies with the pressure of the environment of the sample; it becomes greater as this pressure increase. This phenomenon is seemingly due to the fact that at higher pressure the crystallites of the nano-powder get closer to each other, facilitating the cooperative emission. The existence of this phenomenon suggests the possible use of this system as an optically-based pressure sensor. It is clear that, while the integrated cooperative emission intensity decreased with decreasing pressure from

1 atm to 10^{-2} mbar, the green emission around at 520 nm increase with decreasing pressure.

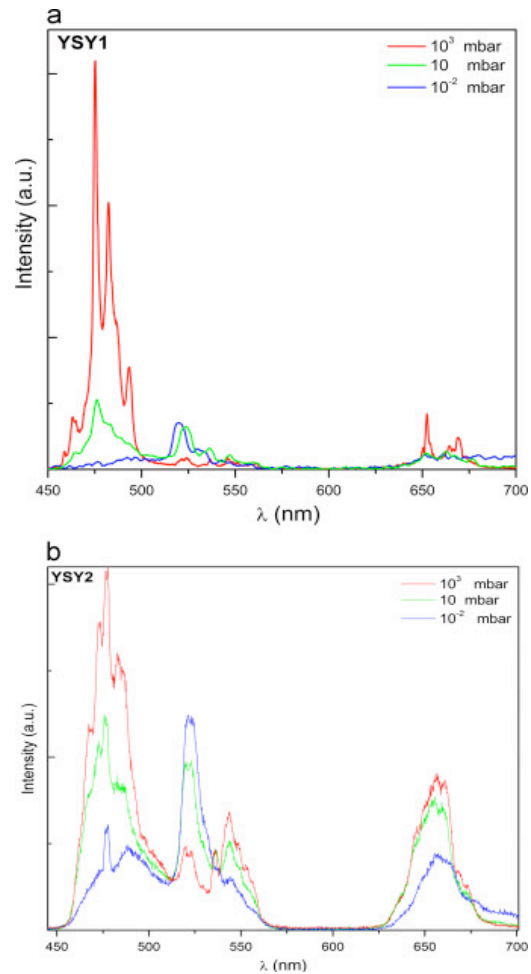


Figure 3 Pressure effects on the cooperative emissions for (a) $\alpha\text{-Y}_2\text{Si}_2\text{O}_7$ and (b) $\gamma\text{-Y}_2\text{Si}_2\text{O}_7$ powders activated with Yb^{3+} powders.

Fig.4 gives the room temperature up conversion emission spectra of YSY1 and YSY2 nano-powders in the visible region under the 950 nm laser diode excitation. The visible blue-green emissions were observed by naked eye in the YSY1 nano-powders more intense than in the YSY2 nano-powders as function of pressure.

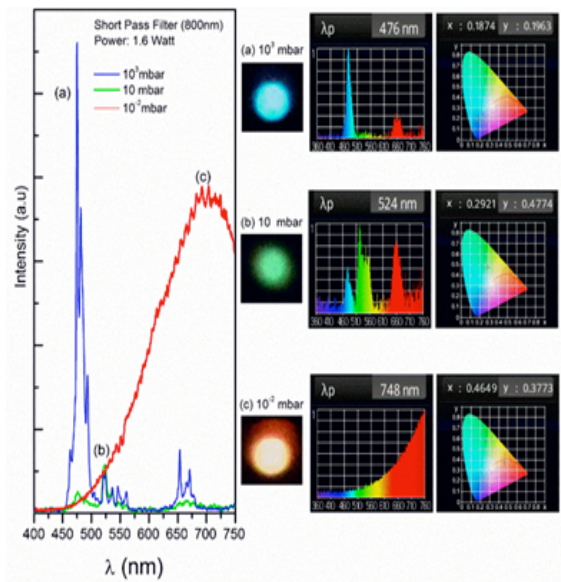


Figure 4 Cooperative emission spectra of the powders measured under different pressures under the 950 nm excitation. (a), (b), (c) are the camera images and the corresponding spectra together with the CIE coordinates of white light measured by an illuminance meter.

The intensity of the UC-luminescence at 476 nm is given in Fig. 5 as function of the pressure. A strong dependence on pressure was observed for the blue emission under the environment pressure of 4×10^2 mbar. Intensity increase with pressure

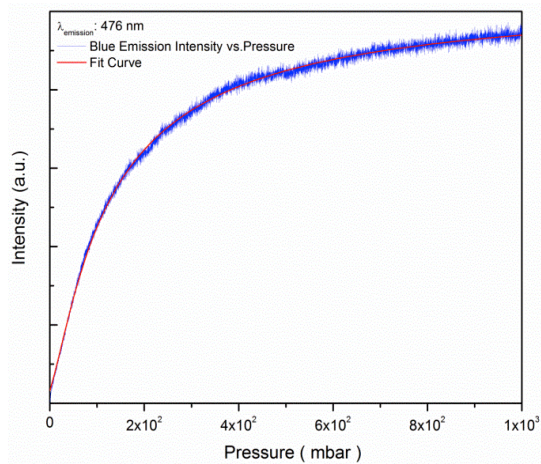


Figure 5 Pressure dependence of the blue UC-luminescence in Yb^{3+} doped Yttrium Silicate nanopowders.

4 CONCLUSION

The ytterbium (Y^{3+}) doped $\alpha\text{-Y}_2\text{Si}_2\text{O}_7$ and $\gamma\text{-Y}_2\text{Si}_2\text{O}_7$ nano-crystalline powders with average particle size 40 and 70 nm were successfully synthesized using the sol-gel technique. Up-converted emission was obtained from the nano-powders on excitation by a 950 nm diode laser. Strong pumping power and ambient pressure dependencies of the cooperative and IR emission were observed. While the blue emission intensities of the spectral lines for the powders decrease with decreasing pressure, the green emission intensities increased with decreasing pressure. The $\alpha\text{-Y}_2\text{Si}_2\text{O}_7$ and $\gamma\text{-Y}_2\text{Si}_2\text{O}_7$ activated with Yb^{3+} , since they present bright blue and green light emission depending on pressure may be useful as optical-based pressure sensors in potential photonic applications.

REFERENCES

- [1] G. Boulon, *J. Alloys Compd.* 451 (2008) 1–11.
- [2] G.Y. Chen, Y. Liu, G. Zhang, G. Somesfalean, Z.G. Zhang, Q. Sun, F.P. Wan, *Appl. Phys. Lett.* 91 (2007) 133103.
- [3] D. Hreniak, P. Gluchowski, W. Strek, M. Bettinelli, A. Kozłowska, M. Kozłowski, *Mater. Sci. Poland* 24 (2006) 405–413.
- [4] L. Marciniak, W. Strek, A. Bednarkiewicz, D. Hreniak, M.C. Pujol, F. Diaz, *J. Lumin.* 133 (2013) 57–60.
- [5] A. Lazarowski, S. Mahlik, M. Grinberg, C.W. Yeh, R.S. Liu, *J. Lumin.* 159 (2015) 183–187.
- [6] S. Mahlik, M. Behrendt, M. Grinberg, E. Cavalli, M. Bettinelli, *Opt. Mat.* 34 (2012) 2012–2016
- [7] S. Mahlik, E. Cavalli, M. Bettinelli, M. Grinberg, *Radiation Measurements* 56 (2013) 1–5.
- [8] M. Erdem, G. Eryurek, A. Mergen, B. Di Bartolo, *Ceram. Int.* 42 (2016) 1501–1506
Compd. 639 (2015) 483–487
- [9] X. Chen, Y. Li, F. Kong, L. Li, Q. Sun, F. Wang, *J. Alloy. Compd.* 541 (2012) 505–509.
- [10] H. Hu, Y. Bai, *J. Alloy. Compd.* 527 (2012) 25–29.
- [11] J.J. Li, L.W. Yang, Y.Y. Zhang, J.X. Zhong, C.Q. Sun, P.K. Chu, *Opt. Mater.* 33 (2011) 882–887.
- [12] M. Erdem, G. Eryurek, B. Di Bartolo, *J. Alloy. Compd.* 639 (2015) 483–487
- [13] A.I. Becerro, A. Escudero, P. Florian, D. Massiot, M.D. Alba, *J. Solid State Chem.* 177 (2004) 2783–2789.
- [14] J. Felsche, *Struct. Bond.* 13 (1973) 99–197.